

This article was downloaded by:

On: 26 January 2011

Access details: *Access Details: Free Access*

Publisher *Taylor & Francis*

Informa Ltd Registered in England and Wales Registered Number: 1072954 Registered office: Mortimer House, 37-41 Mortimer Street, London W1T 3JH, UK



Liquid Crystals

Publication details, including instructions for authors and subscription information:

<http://www.informaworld.com/smpp/title~content=t713926090>

The role of hydrogen bonding on a hydroxylated liquid crystal, bis [4-(5-hydroxypentyl)oxy]phenylene] terephthalate

Chih-Hsiung Lin^a; Yen-Long Hong^a; Fu-Shan Yen^b; Jin-Long Hong^b

^a Department of Chemistry, Institute of Materials Science and Engineering, Kaohsiung, Taiwan, R.O.C

^b National Sun Yat-Sen University, Kaohsiung, Taiwan, R.O.C

To cite this Article Lin, Chih-Hsiung , Hong, Yen-Long , Yen, Fu-Shan and Hong, Jin-Long(1996) 'The role of hydrogen bonding on a hydroxylated liquid crystal, bis [4-(5-hydroxypentyl)oxy]phenylene] terephthalate', *Liquid Crystals*, 21: 5, 609 – 618

To link to this Article: DOI: 10.1080/02678299608032872

URL: <http://dx.doi.org/10.1080/02678299608032872>

PLEASE SCROLL DOWN FOR ARTICLE

Full terms and conditions of use: <http://www.informaworld.com/terms-and-conditions-of-access.pdf>

This article may be used for research, teaching and private study purposes. Any substantial or systematic reproduction, re-distribution, re-selling, loan or sub-licensing, systematic supply or distribution in any form to anyone is expressly forbidden.

The publisher does not give any warranty express or implied or make any representation that the contents will be complete or accurate or up to date. The accuracy of any instructions, formulae and drug doses should be independently verified with primary sources. The publisher shall not be liable for any loss, actions, claims, proceedings, demand or costs or damages whatsoever or howsoever caused arising directly or indirectly in connection with or arising out of the use of this material.

The role of hydrogen bonding on a hydroxylated liquid crystal, bis[4-(5-hydroxypentylcarbonyl)phenylene] terephthalate

by CHIH-HSIUNG LIN, YEN-LONG HONG, FU-SHAN YEN†
and JIN-LONG HONG*†

Department of Chemistry and Institute of Materials Science and Engineering†,
National Sun Yat-Sen University, Kaohsiung, Taiwan, R.O.C

(Received 30 November 1995; in final form 23 May 1996; accepted 25 May 1996)

Hydroxyl-terminated liquid crystalline bis[4-(5-hydroxypentylcarbonyl)phenylene] terephthalate (BHT) was prepared and compared with its non-hydroxylated analog, bis[4-(pentylcarbonyl)phenylene] terephthalate (BPT). BHT, with the possibility to form intermolecular hydrogen bonding (H-bonding), has higher thermal transition temperatures (T_m and T_i) than BPT. Infrared spectroscopy was applied to prove the existence of H-bonding for BHT. An X-ray diffraction study suggests that the smectic A (S_A) phase is the only phase existing for BPT but for BHT, an interdigitated layered structure was found to be mixed with the S_A phase. The formation of this interdigitated layered structure is mainly due to the intermolecular H-bonding between the terminal hydroxyl and the external ester groups in BHT.

1. Introduction

Several arguments concerning hydrogen bonding (H-bonding) as the molecular criterion for mesomorphism (liquid crystallinity) [1-3], in addition to rigidity, rod shape, and polarity [4-6], have been previously presented. The first example, proposed by Gray in 1962 [7], suggested that phenols had never been observed to be mesomorphic because intermolecular hydrogen bonding raises the melting point above the mesophase-isotropic liquid (T_i) transition temperature and may also encourage the formation of a non-linear molecular arrangement. Later, Schroeder reported [1,2], based on the results from 4-(4-hexyloxybenzoyloxy)phenyl 4-hydroxybenzoate and some related compounds, that hydrogen bonding is not detrimental to mesomorphism if the involved mesophase is packed in a well-ordered, parallel fashion. Two possible arrangements of end-to-end and sidewise H-bonding were proposed to explain the observed nematic and smectic mesophases, respectively. To compare, Sakurai *et al.* [3], prepared liquid crystals with the same chemical framework but with a methoxy (or a chlorine) rather than a hydroxyl terminal. In this manner, the effect of H-bonding on thermal properties was evaluated. It was then found that the smectic A (S_A) to nematic (N) phase transition temperature is promoted by H-bonding while the nematic-to-isotropic (I) transition temperature is independent of H-bonding. However, Sakurai suggested that a correlation between H-bonding and the smectic

properties was not available due to the scarcity of observations in other compounds.

The above examples illustrate liquid crystals with hydroxyl terminals attached to a phenylene moiety (i.e., phenol terminal). This hydroxyl terminal is acidic ($pK_a \sim 10$) [8] and its capability of H-bonding is influenced by the neighbouring phenylene group and the linkages (i.e., ester bonds) between the phenylene due to resonance effects. In all cases, the effect of H-bonding should be greatly affected by the incorporated chemical groups and a clear evaluation is basically prohibited. Furthermore, these liquid crystals with phenol terminals generally possess high T_m and T_i [1]; decomposition before mesophase formation usually occurs, obscuring experimental results. To avoid the possible complications mentioned above, a liquid crystal with its hydroxyl group connected to an aliphatic chain, instead of aromatic ring, was used in this study. As suggested by Schroeder [2], H-bonding can enhance mesomorphic stability if the involved phase is a well-organized, layered smectic structure. It is well recognized that a smectic mesophase can be easily introduced by increasing the terminal chain length. Therefore, use of an aliphatic instead of an aromatic hydroxyl terminal has the advantage to study the H-bonding effect in terms of a smectic mesophase. In this study, bis[4-(5-hydroxypentylcarbonyl)phenylene] terephthalate (BHT in scheme 1) is used to evaluate the effect of H-bonding. An analogous compound, bis[4-(pentylcarbonyl)phenylene] terephthalate (BPT in scheme 1), without hydroxyl terminals was also synthesized for purpose of comparison.

*Author for correspondence.

In this study, differential scanning calorimetry (DSC), Fourier-transform infrared spectroscopy (FTIR), and X-ray diffraction (XRD) were all applied in order to evaluate the effect of terminal hydroxyl groups in relation to the resulting mesophase.

2. Experimental

2.1. Materials and instrumentation

Terephthaloyl chloride was recrystallized from hexane. Recrystallization of *p*-hydroxybenzoic acid from distilled water was performed before use. 1,1,2,2-Tetrachloroethane (TCE) was used without purification.

Proton NMR was recorded with a VXR-300 FT-NMR model or a Varian Gemini-200 200 MHz model. Tetramethylsilane (TMS) was used as the internal standard in all cases. A Biorad FTS-40 Fourier-transform infrared spectrometer was used to measure spectra in the optical ranges of 4000–400 cm^{-1} . Compound identifications were performed with KBr pellets for solid samples and CaF_2 pellets for liquid samples. For the temperature-programming study, the sample in a Pyrex holder was sitting in a Pyrex cell (diameter = 25 mm, length = 150 mm) connected to a thermocouple. The study was performed under vacuum. Mass spectroscopy was performed with a Hitachi M-52 model.

The textures of the liquid crystals were observed with a Nikon Optiphot-POL microscope equipped with a Linkam TMS controller and THMS 600 hot stage. Phase transition temperatures were detected with a Du-Pont DSC-910 model connected to a Du-Pont 9900 data station. The carrier gas was nitrogen at a flow rate of $c. 10 \text{ ml min}^{-1}$. Calibration of the calorimeter was conducted for each heating rate using an indium standard. Temperature-programming X-ray diffraction was

performed with a Siemens Diffraktometer D5000 model. The system was evacuated to a pressure of 10^{-5} torr before heating to high temperature. Room temperature X-ray diffraction patterns were recorded on a flat film with an Enraf-Nonius 582 D60 X-ray camera using Cr radiation. Sample preparation was performed as follows: A glass bar of diameter $\sim 0.5 \text{ mm}$ was rolled in molten BHT at 200°C to attach the sample for the test. This stained glass bar was then withdrawn and quenched immediately in liquid nitrogen, and sent for X-ray measurement. Computer modelling was performed using CSC Chem3D (Cambridge Scientific).

2.2. Synthesis

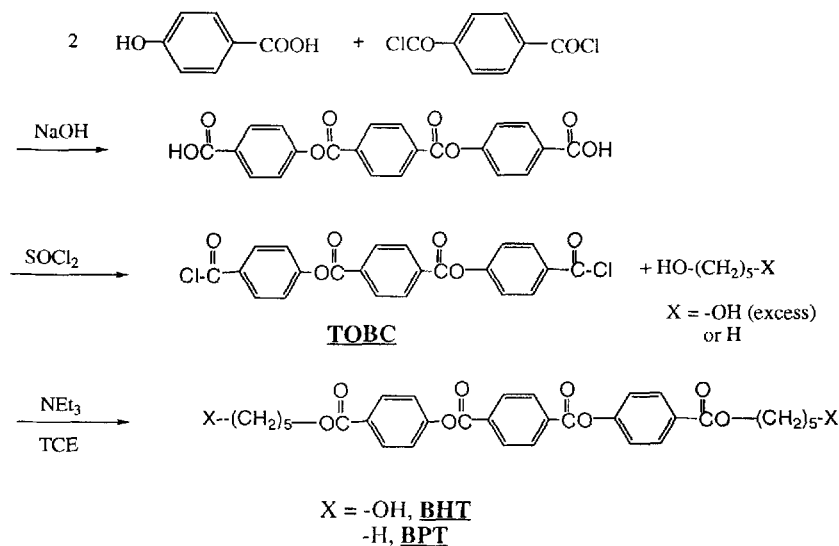
The syntheses of bis[4-(5-hydroxypentylloxycarbonyl)phenylene]terephthalate (BHT) and bis[4-(pentylloxycarbonyl)phenylene]terephthalate (BPT) are briefly illustrated in scheme 1. The detailed synthesis procedures were given below.

2.2.1. Synthesis of bis[(4-benzoylchloride)terephthalate (BCT)]

Synthesis of BCT was performed following the procedures outlined in scheme 1, and described in detail elsewhere [9, 10]. ^1H NMR (200 MHz, d^6 -DMSO): δ 8.35 (s, 4H, aromatic H), 8.08–8.04 (d, $J = 8 \text{ Hz}$, 4H, aromatic H), 7.50–7.46 (d, $J = 8 \text{ Hz}$, aromatic H). m.p.: 223°C .

2.2.2. Synthesis of bis[4-(5-hydroxypentylloxycarbonyl)phenylene]terephthalate (BHT) and bis[4-(pentylloxycarbonyl)phenylene]terephthalate (BPT)

Into a mixture of 1,5-pentanediol (0.3 mol) and 1,1,2,2-tetrachloroethane (TCE, 30 ml), a hot solution of BCT (0.03 mol) in 200 ml of TCE was slowly added



Scheme 1. Syntheses of BHT and BPT.

dropwise. The reaction mixture was then refluxed for 8 h under a nitrogen atmosphere. The resulting solution was then poured into 300 ml of ice-cooled toluene and kept in a refrigerator for 10 h. The white precipitate was filtered, washed with ether and then subjected to a two-layer (aq. NaCl/CHCl₃) extraction. The organic layer was dried over MgSO₄ and the solvent was removed to obtain the final product. BPT was synthesized by reacting 1-pentanol (1.77 ml) with BCT (8.12 mmol) in 60 ml of TCE (60 ml). The reaction mixture was refluxed for 10 h. The resulting hot solution was filtered and precipitated with methanol to obtain a white solid, and extracted with ether to obtain the crude product. The final product was purified by column chromatography with ethyl acetate:hexane (1:3v/v) as eluent. ¹H NMR of BHT (300 MHz, *d*⁶-DMSO): δ 8.36 (s, 4 H, aromatic H), 8.09 (d, 4 H, *J*=10 Hz, aromatic H), 7.53 (d, *J*=10 Hz, 4 H, aromatic H), 4.46 (t, *J*=3 Hz, 2 H, -OH), 4.34 (t, *J*=4 Hz, 4 H, -COOCH₂-), 3.41 (q, *J*=4.3 Hz, 4 H, -CH₂-OH), 1.86-1.80 (m, 4 H, -CH₂-), 1.69-1.52 (m, 8 H, -CH₂-). IR (KBr pellet, cm⁻¹): 3338, 2859, 1736, 1715. Mass (*m/e*): 579 (M⁺). Elemental analysis: theoretical, C 66.43, H 5.92; Found, C 66.14, H 5.87 per

cent. ¹H NMR of BPT (300 MHz, CDCl₃): 8.36 (s, 4 H, aromatic H), 8.16 (d, 4 H, *J*=9 Hz, aromatic H), 7.35 (d, 4 H, *J*=9 Hz, aromatic H), 4.34 (t, 4 H, *J*=4 Hz, -COO-CH₂-), 1.72-1.78 (m, 4 H, -CH₂-), 0.85 (t, 6 H, *J*=5 Hz, -CH₃). IR (KBr, cm⁻¹): 1732, 1722, 1703. Thin layer chromatography: *R_f* (ethyl acetate)=0.63. Mass (*m/e*): 547 (M⁺). Elemental analysis: theoretical, C 70.31, H 6.30; Found, 70.30, H 6.27 per cent.

3. Results and discussion

The synthesis of BHT was performed by reacting BCT with an excess of 1,5-pentanediol (see scheme 1), in such a way as to eliminate the higher molecular weight oligomers. The purity of the resulting BHT was proved by careful examination of the relative peak integrations in ¹H NMR, thin layer chromatography, and elemental analyses as listed in the experimental section. Analogous procedures were performed to synthesize BPT and its DSC thermogram was compared with BHT in figure 1. For BHT, the first two endotherms starting from the low temperature region are two crystal-crystal transitions, which disappeared as BHT was rescanned after quenching from its mesomorphic state (in this case,

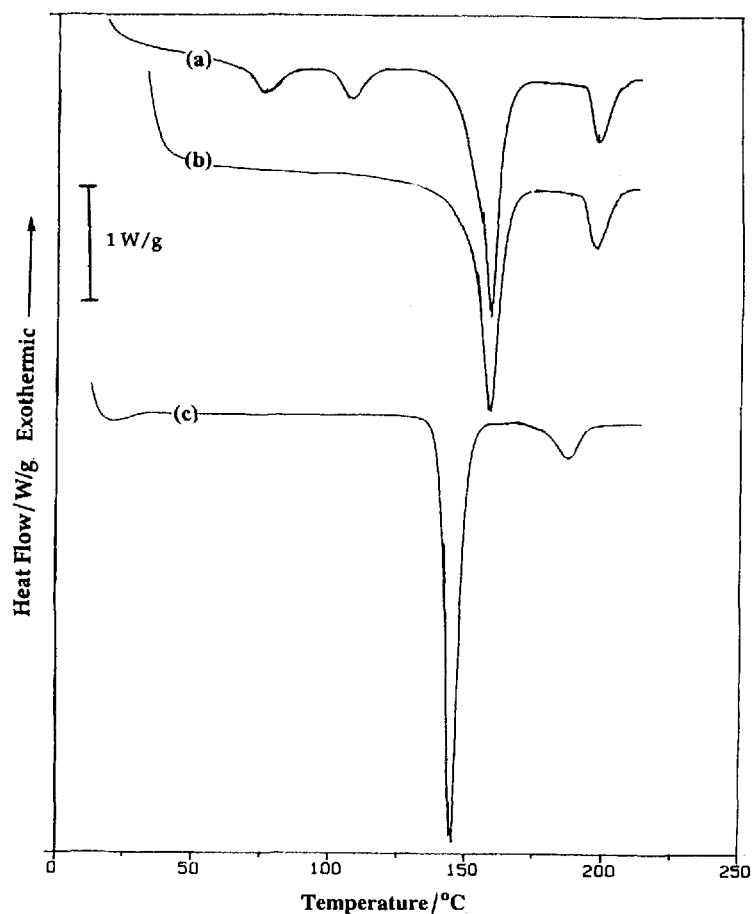


Figure 1. Dynamic DSC scans of (a) BHT (first heating), (b) BHT after quenching from 170°C and (c) BPT at a heating rate of 20°C min⁻¹.

170°C). The resulting thermogram (see figure 1(b)) showed two endotherms representative of melting (T_m) and isotropization (T_i) of BHT, respectively. These two transitions can be visualized as exotherms in the DSC cooling scan, which demonstrates the enantiotropism of BHT. The thermogram of BPT, unlike BHT, exhibits only two endotherms with their corresponding T_m and T_i relatively lower than those of BHT (cf. figures 1(b) and 1(c)). The enthalpies (ΔH_i) and entropies (ΔS_i) associated with isotropization, and the mesomorphic textures observed by POM are summarized in the table. Primarily, based on the study of Dewar and Griffin [11] on different nematic esters, isotropic melting temperatures (T_i) are determined by both the enthalpy (ΔH_i)

and entropy (ΔS_i) changes (i.e. $T_i = \Delta H_i / \Delta S_i$). The involvement of intermolecular H-bonds (either between the -OHs or -OHs and the carbonyl groups) in BHT may be responsible for its higher ΔH_i value as compared to BPT. Also, the possible intermolecular H-bonds in BHT should maintain its mesomorphic state in a more ordered structure than in BPT. BHT is supposed to have a more ordered isotropic liquid state as compared to BPT due to its persistent H-bonding in the corresponding state (confirmed by the infrared result discussed below). Therefore, the actual entropy change (ΔS_i) for BHT in passing from the mesomorphic to the isotropic liquid state should be larger than the experimental value (i.e., $15.53 \text{ J K}^{-1} \text{ mol}^{-1}$). The mesophase of BHT should

Table. Summarized results from the DSC scans and POM.

Compound	T_m^a/K	T_i^b/K	$\Delta H_i^c/\text{kJ mol}^{-1}$	$\Delta S_i^d/\text{J K}^{-1} \text{ mol}^{-1}$	Texture ^e
BPT	417	459	4.69	10.22	Fan-shaped
BHT	431	471	7.33	15.53	Biphasic ^f

^aMelting point from the peak temperature in the DSC thermogram.

^bIsotropization temperature from the peak temperature in the DSC thermogram.

^cEnthalpy of isotropization evaluated from the DSC thermogram.

^dEntropy calculated from $\Delta H_i/T_i$.

^eLiquid crystalline texture observed by POM.

^fCoexistence of an unidentified anisotropic texture and dark domains.

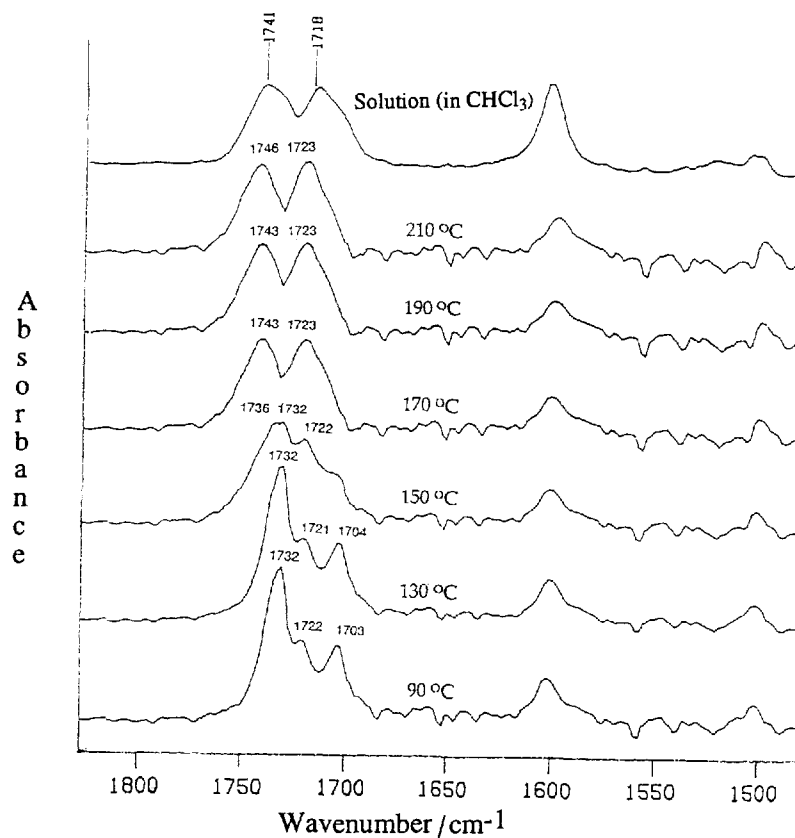


Figure 2. Variations in the carbonyl absorptions for BPT at different temperatures.

be even more ordered than that for BPT. The observed biphasic texture for BHT is related with by XRD study and will be discussed following this section.

Selective absorption regions of the infrared spectra for BPT and BHT at various temperatures are given in figures 2 and 3 respectively. The variations in the carbonyl absorption for BPT in its crystalline and mesomorphic states resemble those of an analogous compound, $\text{CH}_3(\text{CH}_2)_9\text{-OOC-C}_6\text{H}_4\text{-OOC-C}_6\text{H}_4\text{-COO-C}_6\text{H}_4\text{-COO-(CH}_2)_9\text{CH}_3$ reported by Galbiati [12,13]. Detailed discussion for the peak assignment is given in [11] and a related report by Jones [14], which will not be repeated here. For BPT at 90°C , the 1732 cm^{-1} absorption is attributed to the two internal carbonyl ($-\text{Ar-COO-Ar}-$) groups while the absorptions at 1722 and 1703 cm^{-1} are due to the external carbonyl

($-\text{Ar-COO-R}-$) groups. It is assumed that the two external carbonyl absorptions are caused by the dipole-dipole interactions (or different crystal forms present in the solid state, an argument that had not yet been concluded by Galbiati [13]) between neighbouring carbonyl groups in the solid state. Upon heating to the mesomorphic state, the intensity of the 1703 cm^{-1} peak gradually decreased with an increase of peak intensity at 1722 cm^{-1} . These two external absorptions remained at these wavelengths positions after melting and isotropization, indicating intermolecular interactions between external carbonyls are not changed. On the contrary, absorption at 1732 cm^{-1} shifted to a higher frequency as BPT was heated into its mesomorphic and isotropic states, indicating a change in the conformation of the internal $-\text{O-Ar}-$ bonds. Absorption patterns in the

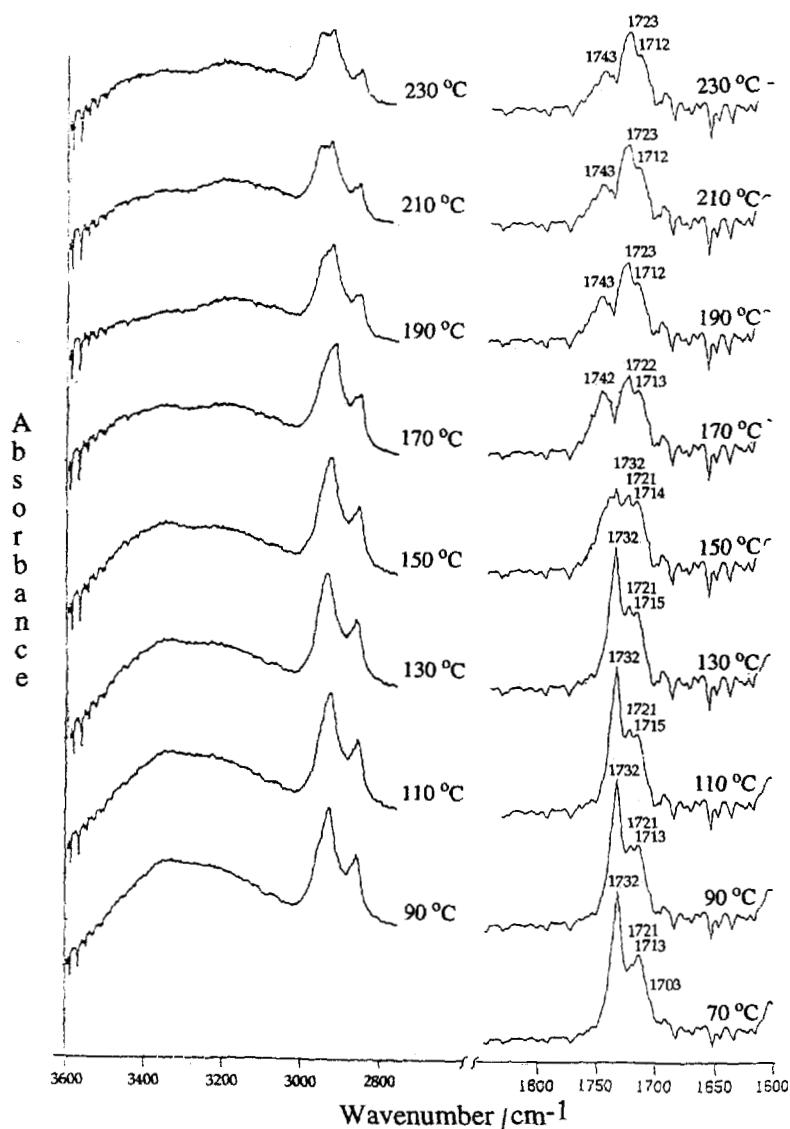


Figure 3. Variations in the hydroxyl (right part) and carbonyl absorptions for BHT at different temperatures.

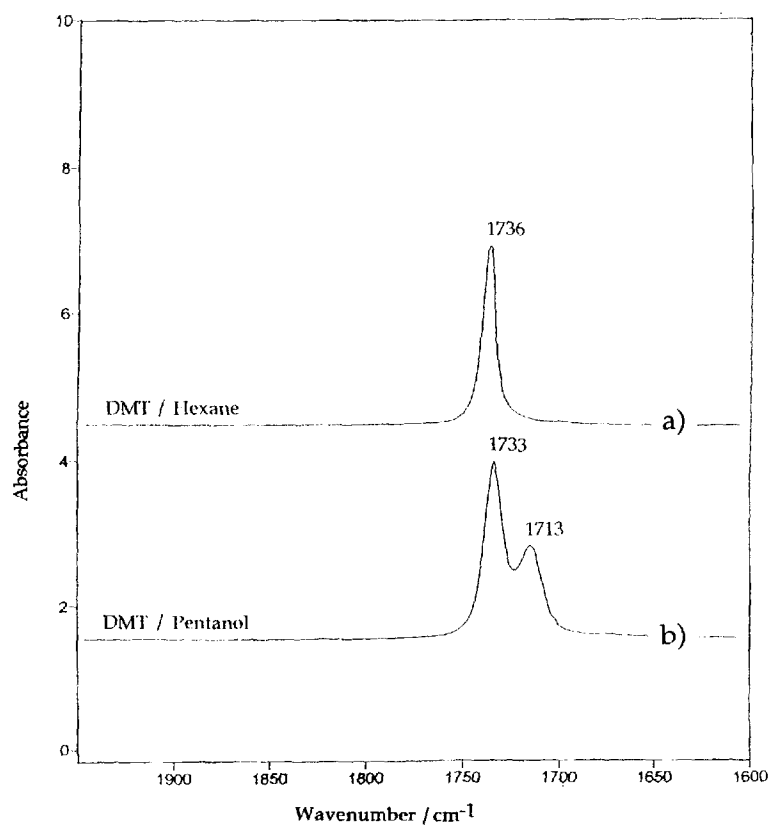


Figure 4. Carbonyl absorptions for DMT in (a) hexane and (b) pentanol.

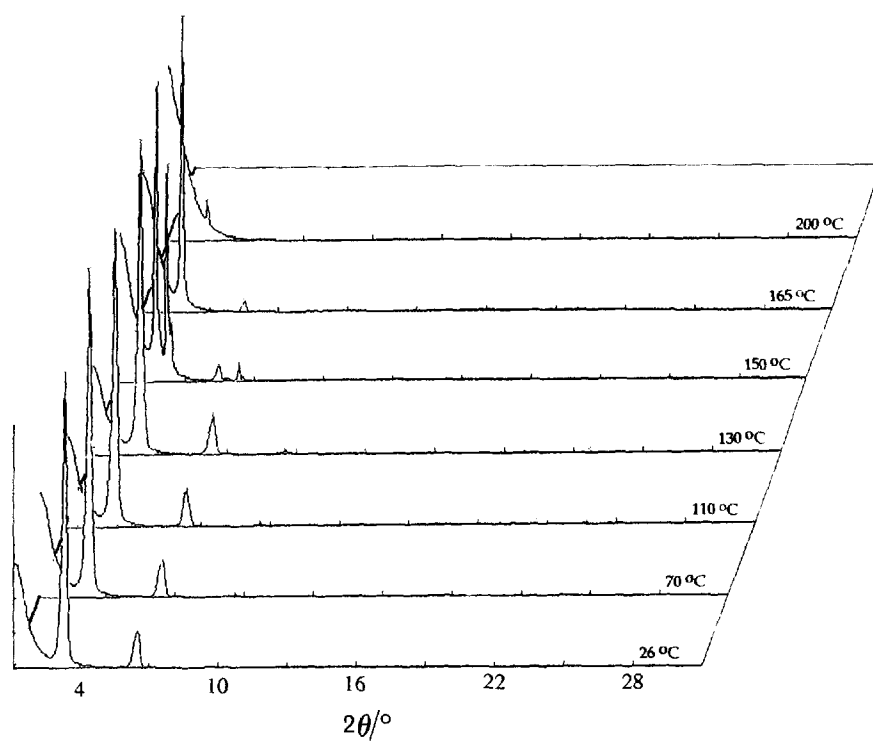


Figure 5. X-ray diffraction patterns for BPT at different temperatures.

mesomorphic and isotropic states are essentially the same, a phenomenon that had been previously observed by Galbiati [12]. This suggests that the isotropic phase consists of a collection of microdomains whose directors are randomly oriented but inside the microdomains, the molecules are organized as they are in the smectic phase. The incapability of FTIR to distinguish the mesophase from the isotropic phase suggests that the vibrational spectra are only good as probes for intermolecular interactions at short range [13]. Comparative spectra of BHT (in figure 3) at $T \leq 130^\circ\text{C}$ basically resemble those of BPT except the main lower absorption is located at 1713, instead of at 1703 cm^{-1} in this case.

Presumably, this 1713 cm^{-1} absorption is due to the H-bonded carbonyl ($-\text{Ar}-\text{COO}-\text{R}-$) groups. Evidence for this 1713 cm^{-1} peak as a H-bonded carbonyl absorption can be obtained from the FTIR study of two related compounds, dimethyl terephthalate (DMT) and bis(5-hydroxypentyloxy) terephthalate (HT), synthesized in our laboratory. DMT exhibited one sharp carbonyl absorption at 1720 cm^{-1} ; while for HT, except for a

1719 cm^{-1} absorption, an intense peak at 1713 cm^{-1} was observed in its IR spectrum. Further confirmation can be sought by comparison of the IR spectra of DMT in hexane and pentanol (see figure 4), respectively. The extra 1713 cm^{-1} peak in figure 4(b) is attributed to the H-bonding interactions between the carbonyl groups of DMT and hydroxy groups of pentanol. For BHT, the peak at 1703 cm^{-1} was hidden as a small shoulder on the 1713 cm^{-1} peak. Upon heating into the mesomorphic state, BHT behaves similarly to BPT but here, the intensity of the 1723 cm^{-1} absorption (free external carbonyl) became the most intense. It is rationalized that certain portions of the external carbonyl groups are H-bonded in the solid state and become free if transformed into the mesomorphic liquid state. Interestingly, this H-bonded carbonyl absorption still persists at temperatures higher than T_i . This may also correspond to the fact that, as Galbiati [12] suggests, the isotropic phase is a collection of microdomains whose directors are essentially organized as they are in the smectic phase. We also suggest the prevalence of H-bonds in the

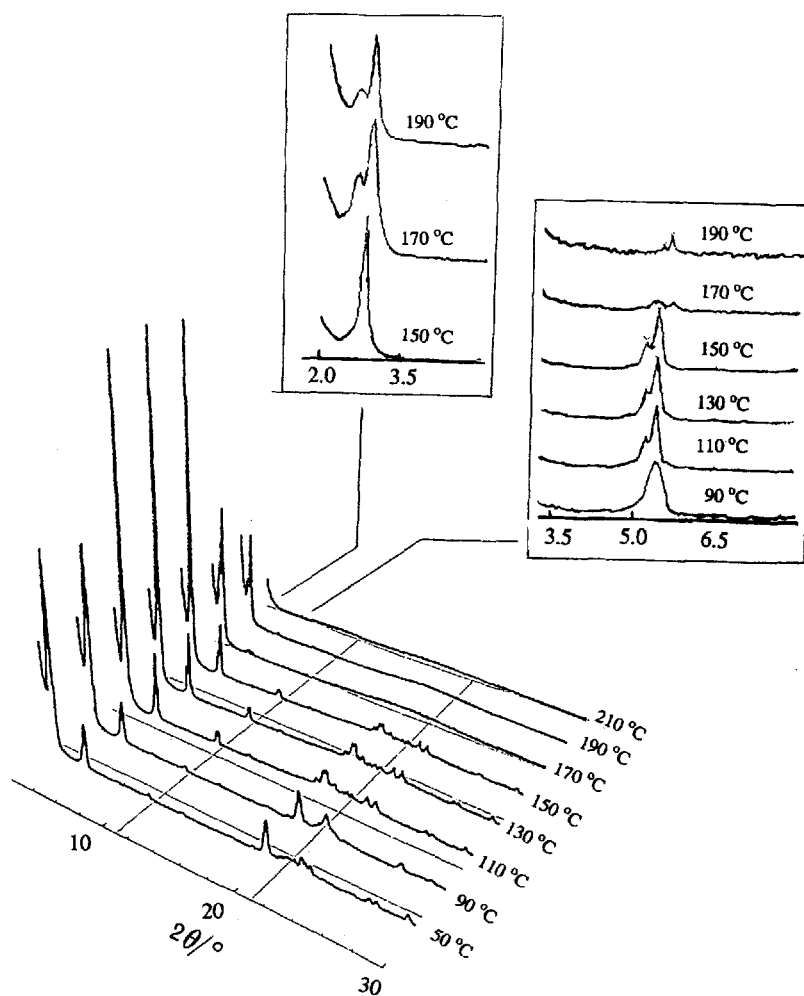


Figure 6. X-ray diffraction patterns for BHT at different temperatures. (The enlarged portions in the small angle region are included in the upper left corner.)

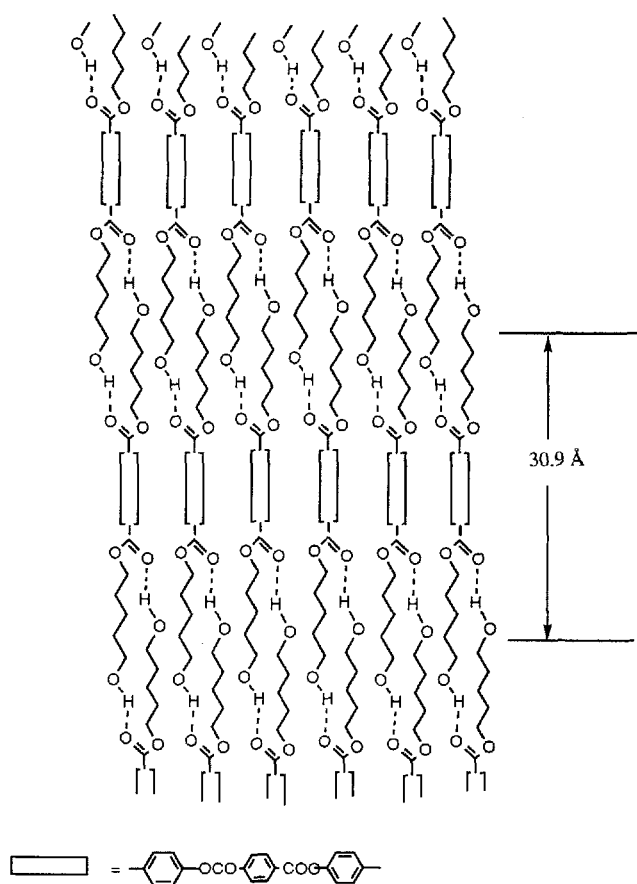


Figure 7. The proposed interdigitated structure for BHT in its mesomorphic state. (The dashed line indicates the H-bonds between $-OH$ and outer carbonyl group; the stick-and-ball model shown on the lower right corner was simulated from Chem3D plus.)

isotropic state by checking the $-OH$ absorptions, shown in figure 3. The increase of bonded OH (centred around 3200 cm^{-1}) relative to free OH (around 3350 cm^{-1}) indicates the important role of hydrogen bonding in the isotropic state of BHT. The bonded OH , of course, may be caused by the H-bondings among terminal OH s or between OH s and carbonyl groups; a point cannot be clearly distinguished at the present time.

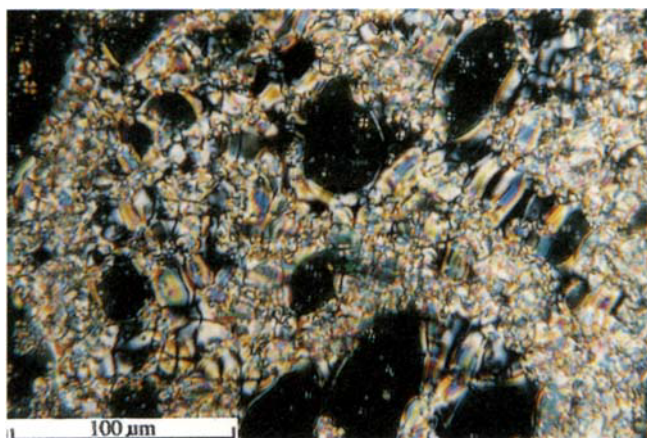
Molecular arrangements for both BPT and BHT can be explored by XRD performed at various temperatures. The resulting diffraction patterns for BPT are plotted in figure 5. The patterns show the profound change when BPT was transformed from its crystalline to mesomorphic state. At 165°C , BPT exhibits two sharp peaks at $2\theta = 2.72$ and 5.34° , corresponding to a d -spacing of 32.5 and 16.5 \AA , respectively. The calculated molecular length of BPT is 32.3 \AA , close to the experimental value (i.e. 32.5 \AA). The peak at $2\theta = 5.34^\circ$ corresponds to a d -spacing equal to half the molecular length, which is

probably due to the centrosymmetrical structure of BPT. A S_A mesophase is therefore assigned for BPT. For BHT, the broad diffraction at $2\theta \sim 5.3^\circ$ transformed into two distinguishable peaks centred at $2\theta = 5.20$ and 5.35° (see figure 6) when the sample was heated from 90 to 110°C . This phenomenon is supposed to be connected with the two crystal-crystal transitions observed in the DSC thermogram (cf. figure 1(a)) described above. At 170°C , these two peaks almost disappeared and instead, the diffraction peak at the lower angle ($2\theta \sim 2.7^\circ$) changed from a broad peak (probably two superimposed peaks) into two distinct peaks at $2\theta = 2.62$ and 2.88° , respectively. Two sets of doublet peaks can be easily seen from the enlarged patterns shown on the upper right side of figure 6. Further heating to 230°C resulted in a broadening of all peaks. Analogously, a S_A mesophase can be applied to BHT to account for the d -spacings at $2\theta = 2.60^\circ$ ($=33.9\text{ \AA}$) and 5.43° ($=16.3\text{ \AA}$) in figure 3; nevertheless, the presence of the extra peaks at $2\theta = 2.85^\circ$ ($=30.9\text{ \AA}$) and 5.57° ($=15.8\text{ \AA}$) suggests the formation of another mesomorphic state for BHT. An interdigitated layered structure (see figure 7) was proposed to interpret the observed diffraction patterns at $2\theta = 2.85$ and 5.57° . Accordingly, the half spacing of 15.8 \AA was due to the centrosymmetrical structure of this interdigitated layered structure. Previously, several low molecular weight liquid crystals with strong longitudinal dipole moments [15] (as in the case if the molecular terminal group is CN or NO_2) were found to exist in an interdigitated bilayered structure in their corresponding mesophases since the interaction between neighbouring dipole moments favours an antiparallel arrangement. The situation is different for BHT since it bears no such polar groups and the only source of interaction may come from the H-bonding between terminal $-OH$ and carbonyl groups as depicted in figure 7. This lateral, intermolecular H-bonding between the $-OH$ and outer ester group in BHT contributes to the formation of an interdigitated layered mesophase, which coexists with the S_A phase.

Infrared spectroscopy can be used to explain the role of H-bonding in BHT. The IR spectra in figure 3 suggests that H-bondings between the $-OH$ and external carbonyl groups exist in the interdigitated layered structure and even persists into the isotropic liquid state. Also, the coexisting S_A phase should also possess H-bonds among the terminal $-OH$ s, which exist mostly on the layer surface. Thomas had previously studied the H-bonding ability between $-OH$ and a different acceptor [16]. A general sequence in terms of acceptor strength decreases in the order of $-C=O > -NO_2 > -S=O_2 > -C-OH > -C-O-C$. This suggests that the above-mentioned interdigitated structure may be even more stable than the regular S_A phase. We also anticipate that sliding

between layered molecules would facilitate the transformation between these two microstructures. This postulate is, however, unlikely in considering the relatively intact H-bonded carbonyl absorption at 1713 cm^{-1} in passing from the mesomorphic to isotropic state.

POM provided certain evidence for the two mesophases described above for BHT. Figure 8(a) shows that BHT, in its mesomorphic state, exhibits an unfamiliar anisotropic texture accompanied by several dark domains under polarized light. Presumably, these dark domains belong to a homeotropic smectic phase, generated from the H-bond interactions between the $-\text{OH}$ groups in BHT and in the surfaces of the glass slides holding the BHT sample. These dark domains were destroyed by pressing the cover glass. The surface interaction can be avoided if a PET (poly(ethylene terephthalate)) film was used as the cover slide instead of glass. Figure 8(b) shows the resulting fan-shaped texture,



(a)



(b)

Figure 8. (a) The biphasic texture of BHT at 163°C when sample was held between glass slides and (b) the smectic texture of BHT at 180°C when sample was held between PET films.

which, in contrast to figure 8(a), is homogeneous in nature and exhibits no trace of dark homeotropic domain. This homeotropic orientation can be further demonstrated by an X-ray diffraction pattern, shown in figure 9. In this case, the BHT sample was directly quenched from its mesomorphic state on a thin glass bar. The sketch at the top illustrates the geometrical arrangement of the experimental set-up, in which the glass bar holding the sample was perpendicular to the incident X-ray beam. The resulting equatorial scatterings clearly suggest that interactions between $-\text{OH}$ s in BHT and the glass surface directly induced the homeotropic

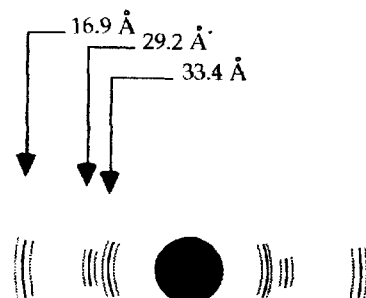
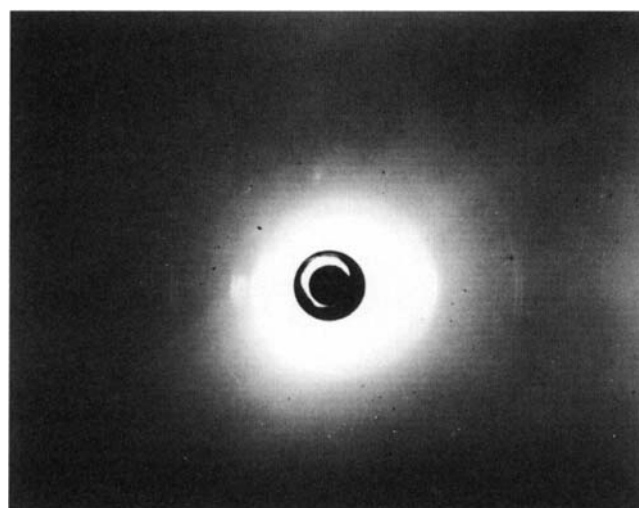
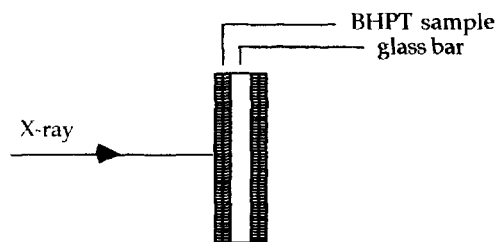


Figure 9. (a) Transmission pin-hole photograph for BHT and (b) duplication of the resulting pin-hole photograph. (The sketch on the top indicates the geometrical arrangement of the test specimen and the incident X-ray beam.)

arrangements. The corresponding d -spacings are approximately close to those obtained by diffractometry (cf. figure 6); except that the $2\theta = 5.57^\circ$ ($d = 15.8 \text{ \AA}$) scattering was missing in this case due to its low intensity.

4. Conclusions

Hydroxyl-terminated bis[4-(5-hydroxypentyl)oxy-carbonyl]phenylene]terephthalate (BHT) was prepared to compare with its non-hydroxylated analogue, bis[4-(pentyl)oxy-carbonyl]phenylene]terephthalate (BPT). BPT, without intermolecular H-bonds, possesses only a S_A phase as evidenced from the X-ray study. On the contrary, BHT, with the inherent H-bonding possibilities between the $-\text{OH}$ and carbonyl groups (or $-\text{OH}$), possesses both S_A phase and an interdigitated layered structure coexisting in the mesomorphic state.

We appreciate the financial support of the National Science Council, R. O. C., under contract no. NSC 84-2216-E-110-008.

References

- [1] SCHROEDER, D. C., and SCHROEDER, J. P., 1974, *J. Am. chem. Soc.*, **96**, 4347.
- [2] SCHROEDER, D. C., and SCHROEDER, J. P., 1976, *J. org. Chem.*, **41**, 2566.
- [3] SAKURAI, Y., TAMATANI, A., TESHIMA, K., and KUSABAYASHI, S., 1992, *Mol. Cryst. liq. Cryst.*, **213**, 163.
- [4] BROWN, G. H., and SHAW, W. G., 1957, *Chem. Rev.*, **57**, 1049.
- [5] SAUPE, A., 1968, *Angew. Chem., Int. Ed. Engl.*, **7**, 97.
- [6] GRAY, G. W., 1976, *Advances in Liquid Crystals*, Vol. 2, edited by G. H. Brown (Academic Press), p. 1.
- [7] GRAY, G. W., 1962, *Molecular Structures and the Properties of Liquid Crystals* (Academic Press), p. 162.
- [8] KEMP, D. S., and VELLACCIO, F., 1980, *Organic Chemistry* (Worth Publishers, Inc.), p. 699.
- [9] BILIBIN, A. Y., TEN'KOVSTEV, A. V., PIRANER, O. N., and SKOROKHODOV, S. S., 1984, *Polym. Sci. U.S.S.R.*, **26**, 2882.
- [10] DIMIAN, A. F., and JONES, F. N., 1988, *Cross-linked Polymers, Chemistry, Properties, and Applications*, edited by R. A. Dickie, S. S. Labana and R. S. Bauer (ACS), p. 324.
- [11] DEWAR, M. J., and GRIFFIN, A. C., 1975, *J. Am. chem. Soc.*, **97**, 6662.
- [12] GALBIATI, E., ZERBI, G., BENEDETTI, E., and CHIELLINI, E., 1991, *Polymer*, **32**, 1555.
- [13] GALBIATI, E., ZOPPO, M. D., TIEGHI, G., and ZERBI, G., 1993, *Polymer*, **34**, 1806.
- [14] JONES, N., 1956, *Techniques of Organic Chemistry*, edited by A. Weissberger (Wiley Interscience), Vol. IX.
- [15] NOEL, C., 1992, *Liquid Crystal Polymers: from Structures to Applications*, edited by D. Acierno, W. Brostow and A. A. Collyer (Elsevier Applied Science), p. 53.
- [16] THOMAS, S., 1994, *J. chem. Soc., chem. Commu.*, **20**, 2341.